

# 4-Stroke Port Injected Turbocharged Snowmobile Design Clean Snowmobile Challenge 2016 Design paper

Marc-Adrien Boyer, Marc-Antoine T. Fitzgerald, Pierre-Olivier Langlois,  
Mathieu Proulx, Paul Raymond, Guillaume Verner  
École de technologie supérieure (ÉTS)

Copyright © 2012 SAE International

## ABSTRACT

As engineering students from the snowmobile's origin province, Team QUIETS has decided to take on the challenge of modifying and improving the image of this vehicle. With growing concerns regarding emissions controls and noise from recreational vehicles such as the snowmobile, we are using a 2012 Ski-Doo 600 ACE 4 stroke engine for our researches. Our modifications include the implementation of a turbocharger, an entirely redesigned exhaust system, an EGR system and a new engine management system in order to improve exhaust emissions and noise reduction. These changes allow our snowmobile to surpass the stock engine power output while being quiet and economic. The modified snowmobile now has a peak power output of 83 horse power (HP) and 63 foot pounds (ft-lbs) of torque at 7000 RPM. Many other modifications concerning the rest of the vehicle will also be presented. This student club is a great example of what a group of 22 students with common goals can accomplish.

## INTRODUCTION

Team QUIETS is proud to present our 2016 Clean Snowmobile Challenge submission. This year, we are pushing further the turbocharged 4-stroke Otto cycle engine design. We believe that this will allow us to achieve the great handling and acceleration characteristics we enjoyed with the two-stroke engine, with much more reliability, while considerably reducing emissions and noise. We also believe that this year's project is considerably more economically viable than its predecessors, as it relies more on stock components and high-value modifications. We have accomplished a lot in a relatively short time, and we look forward to show our improvement at the CSC 2016.

## SNOWMOBILE BASE CHASSIS SELECTION

### **Rev-XS**

One of the biggest improvements we made this year is to update our chassis. Since our previous platform was a 2011 Rev XP, its utility life for the purpose of the competition was coming to an end. We decided to take advantage of the great handling improvement that BRP introduced in the 2016 Rev-XS chassis.

We decided to choose the Ski-Doo MXZ Blizzard as our new platform because it was the best value for us from BRP. It comes with a lot of exclusive options and accessories that will be useful for us (more on that). Another good argument that lead us to this model was that most of the modifications that we made on the previous prototype could be transferred easily.

### **rMOTION suspension**

One of the most significant upgrade over our past setup is the rMOTION suspension that is installed from the factory on the MXZ Blizzard. The rMOTION suspension gives the rider better maneuverability and comfort due to separate spring and shock dynamics that are paired with a fully adjustable system that lets the user tune the suspension as he likes it, either for better comfort, or more response from the snowmobile. Separate dynamics helps to reduce the impact on small bumps, and increase the capability of the suspension on bigger impact.

### **129" track**

One of the biggest changes on the REV-XS chassis was the new 129" track, instead of the initial 121" we had previously. In order to try to compensate from the added drag of the longer track, we chose to reduce the length of the lugs from 1.6" down to 1.25". Since the added length of the track provides an increase in traction, we think the snowmobile will have an overall similar cornering behavior to a shorter track model with taller lugs. On a different note, a longer track gives the snowmobile better stability especially at high speed on

straight trails. It also provides better traction on acceleration/braking in every kind of snow and even more on un-packed snow.



Figure 1. Rev-XS Chassis and rMOTION Suspension

### Pilot TS skis

BRP introduced the Pilot TS skis on some of their 2016 snowmobiles, and we took advantage of it. This feature gives the rider the ability to adjust the depth of the runners in the snow, providing better control in any situation. The driver can therefore choose which settings suits the conditions best and adjust the skis by only having to turn a knob.



Figure 2. New Pilot TS Skis With Adjustment Knob

### Cooling system

Another important aspect considered in our 2016 chassis selection was the larger and improved cooling system offered on the 2016 BRP MXZ blizzard. This newer snowmobile model is equipped with a 7"  $\frac{3}{4}$  by 55" heat exchanger under the chassis bed instead of our previous 7"  $\frac{3}{4}$  by 47". An additional 6" by 12" heat exchanger is standard on the selected Blizzard chassis model. This heat exchanger is installed horizontally under the chassis' tunnel and is not available on the sport chassis. This revised cooling system is also designed to reduce ambient heat in the engine compartment thanks to the 6" by 12" heat exchanger placed behind the engine. The heat that dissipates from the oil pan is absorbed in part by this exchanger. Using this cooling system insures greater reliability from our higher output engine in any winter weather conditions.

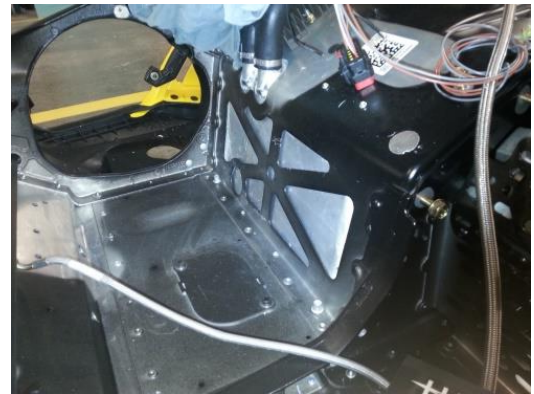


Figure 3. Engine Compartment Heat Exchanger

## ENGINE DESIGN AND MODIFICATIONS

### Engine comparison and selection

The snowmobile engine selection had to follow our objectives. We were looking for a small light engine block with good fuel economy and the reliability to withstand harsh engine calibration. With the help of forums on behalf of the FCMQ (Federation of Snowmobile Clubs of Quebec), we were able to determine the needs of the rider. Environmental issues are not a big concern in the region of Quebec, the main attraction from the buyer's point of view is power and fuel economy. Usually, these two qualities do not go hand in hand, but with the use of a small turbo charged engine block, buyers could get a good compromise on both desires; peak power and great throttle response, as well as good fuel economy while cruising. Theoretically, a 600 Ace turbocharged will have a better fuel economy then its older brother, the 900 Ace, which is a naturally aspired engine. Going for a small turbo charged engine pushes the snowmobile industry to follow the automotive industry where we can witness a rising amount of models available with smaller turbo charged engine blocks with better fuel economy. In order to cope with the added cylinder pressures caused by a turbocharger, we have reduced the compression of the engine from 12.0:1 down to 9.5:1 using a laser cut shim.

Table 1. Engine Comparison

	900 Ace	E-tec	600 Ace Turbo
Displacement	900 cc	600 cc	600 cc
Type	4 Stroke	2 Stroke	4 Stroke
Hp	90	121	83
Fuel Consumption	23 mpg	21 mpg	24 mpg

## Engine Control and Calibration

For the 2016 edition of the CSC we upgraded our engine management computer (EMC) to a Motec M400. We chose Motec because of the proven reliability of the platform in many racing applications over the past years.

The Motec M400 offers features that are very interesting from a calibration standpoint. These include lambda closed loop control, high speed data logging, boost control and many more. By switching to the M400 we also benefit from added functionalities such as the ability to create custom fuel and ignition compensations for different situations. We are also able to fully control our electronic throttle system.

Another important aspect of our decision to switch to Motec is the easy access to technical support. The company's technical support was extremely helpful and we had answers to our questions very quickly. After consulting our school's formula SAE team, which also uses Motec, it seemed obvious this EMC was the one to choose for our prototype.

We believe that completely replacing the snowmobile's EMC gives us an important degree of flexibility in our projects. The unfortunate consequence is that, for the first year at least, one of the largest and most important tasks for our team is the calibration of the engine. The engine calibration has to be perfect in order to avoid damaging the engine with the high amount of heat and added intake pressure caused by the turbo. Our task was greatly assisted by the embedded closed loop lambda control system as seen on figure 4.

Lambda Table (Lambda)		RPM	500	1500	2500	3500	4000	4500	4750	5000	5250	5500	6000	6500	7000
Load kPa	180.0	0.85	0.85	0.85	0.85	0.85	0.85	0.85	0.85	0.84	0.84	0.82	0.82	0.82	0.82
	160.0	0.90	0.90	0.90	0.90	0.90	0.90	0.88	0.88	0.88	0.86	0.84	0.84	0.84	0.84
	150.0	0.95	0.95	0.95	0.95	0.95	0.92	0.92	0.92	0.92	0.90	0.88	0.88	0.88	0.88
	140.0	1.00	1.00	1.00	1.00	1.00	0.95	0.95	0.95	0.95	0.92	0.92	0.90	0.90	0.90
	130.0	1.00	1.00	1.00	1.00	1.00	1.00	1.00	1.00	1.00	0.95	0.95	0.95	0.95	0.95
	120.0	1.05	1.05	1.05	1.05	1.05	1.05	1.05	1.05	1.05	1.00	1.00	1.00	1.00	1.00
	110.0	1.05	1.05	1.05	1.05	1.05	1.05	1.05	1.05	1.05	1.05	1.05	1.05	1.05	1.05
	100.0	1.05	1.05	1.05	1.05	1.05	1.10	1.10	1.10	1.10	1.10	1.10	1.10	1.10	1.10
	80.0	0.00	0.00	1.05	1.05	1.10	1.10	1.10	1.10	1.10	1.10	1.10	1.10	1.10	1.10
	60.0	0.00	0.00	0.00	1.05	1.10	1.10	1.10	1.10	1.10	1.10	1.10	1.10	1.10	1.10

Figure 4. Lambda Table (Engine Load vs RPM)

## Calibration Strategy

Running the engine at a stoichiometric ratio of 1.00 for Lambda is theoretically ideal for maximum efficiency and emissions control. But to maximize fuel economy, a lean combustion is required. Since we are using EGR, we can also commit to a leaner burning engine, since we can compensate for the added NOx. To save on fuel, the programmed closed loop AFR target during cruising speed will rise to 1.05, meaning that between 4500 and 5250 RPM and between a

TPS position of 15 to 20%, the engine will be running on a lean air/fuel mixture (boxed in red on Figure 1).

The programmed AFR value was calculated with the help of the brake specific fuel consumption (BSFC) in g/KW-hr represented by the equation (1).

$$BSFC = \frac{m}{P} \quad (1)$$

Where m is the fuel flow in g/h and P is the engine's power output in kW. On a test bench, while keeping the engine at a constant speed and load, it is possible to witness the variation of the BSFC by changing the AFR. Testing various ratios will plot the curve seen on figure 5. A lower BSFC yields better fuel economy.

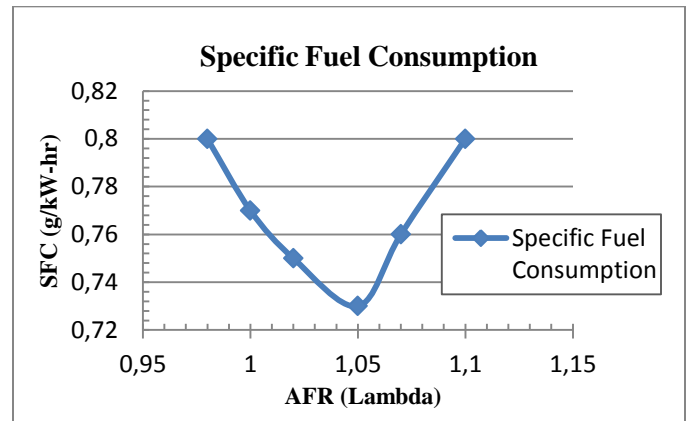


Figure 5. Engine's Specific Fuel Consumption

So by following this curve, we can establish the correct AFR for each operation point running with a lean air/fuel mixture.

As you can see on Figure 1, the aim combustion mixture is lean in most areas where power demands are low. The engine runs above lambda 1.00 when the engine is off boost as well as when it's running at a low boost pressure. However, when boost pressure increases, the mixture is richened in order to preserve the engine and keep the temperatures low. This also allows us to keep ignition advance to a maximum and therefore tuning nearest to maximum brake torque as possible.

By leaning out the map in off boost situations we encourage the engine to build boost when the demand increases. This is particularly useful for us since we have reduced the compression of the engine. In order to match and surpass the efficiency of the stock engine, the engine has to pump more air than it does in its original form. This is achieved using the turbo, which forces the air into the cylinders, thus increasing efficiency. Therefore, it seems logical to force the engine to build boost during cruising conditions, where fuel economy is most important. This being said, with an optimal BSFC as well as a small amount of boost, fuel economy should match or surpass that of the stock engine, while also achieving better emissions.

## Calibrating with Ethanol

The addition of ethanol to the fuel used at the competition this year poses an interesting challenge when it comes to calibration. The specific energy of an 85% ethanol and 15% gasoline blend (E85) being about 30% lower than that of gasoline, the quantity that must be injected to achieve the same power output is increased by roughly 30%. Also, the fact that ethanol chemically contains Oxygen (whereas gasoline doesn't) makes for a lower stoichiometric ratio, 9.78:1 for E85 and 14.7:1 for gasoline.

However, this also has its advantages. By vaporizing a larger quantity of liquid, the heat absorbed during the reaction is also greatly increased, therefore reducing the temperature of the mixture. Colder air is denser air and so the ignition timing can be increased as the risk of pre ignition is reduced with colder air. Thus, the combustion can produce more power with the same amount of fuel than with a warmer mixture, increasing the efficiency of the engine. This also has for effect to lower combustion heat and pressure, which are significant advantages when using a turbocharged engine. Lower exhaust temperatures mean better thermal management (more on that later) and lower cylinder pressures mean the engine can accept more boost, once again increasing efficiency. Ethanol also has a higher octane rating than gasoline, typically around 94-96 AKI for E85. Once again, more power can be made.

In our case, since the ethanol content in the fuel is unknown, a flex fuel sensor must be used to measure the percentage of ethanol in the fuel. Our calibration was done using pump gasoline with a measured ethanol content of 7%. Once the expected results were achieved, we used several blends of ethanol to properly tune our compensation curve. Starting with E85, we also tested with E60, E45, E30 and E20. Though the curve resembles a linear extrapolation, the exercise was worth the effort as a linear compensation would not have been perfectly accurate. The ignition timing compensation has also been adjusted in the same manner. As much as 6 degrees of increased timing has been added in some areas. This has a direct influence on the power our engine produces. As shown on the graph in Appendix A, in the same operating conditions, as much as 14% more power is produced with the same boost pressure, when using E85. In optimal conditions, our engine will achieve a maximum power output of 83hp at 7000 RPM and 63 ft-lb of torque at 5500 RPM.

While not providing as much gain as with E85, lower ethanol content fuels have the same effect but at a smaller scale. They remain promising as an alternate fuel over pure gasoline whatsoever.

## Engine Emissions Control

Regarding emissions found in exhaust gases, only three types of particles really cause a problem for 4 stroke engine. According to EPA standards, our engine should pass a 5-mode resulting in an E-score greater or equal to 175. According to the following formula:

$$E = \left(1 - \frac{(HC + NO_x) - 15}{150}\right) * 100 + \left(1 + \frac{CO}{400}\right) * 100 \quad (2)$$

The compilation of the measured brake specific emissions (g/Kw-hr) of HC, NO<sub>x</sub> and CO will require a score greater than 175. To accomplish this goal our team has opted to implement two types of emissions control systems. Since most of the engine's operating areas aim for a lean burn between lambda 1.00 and 1.10, most of the exhaust gas emissions can be treated with a three way catalyst. A catalyst composed of a stainless steel casing and of a stainless steel substrate from Emitec with coated layers of platinum, rhodium and palladium is used (the detailed analysis of the catalyst selection is presented later in this paper). This single bed three-way catalytic converter system offers conversion efficiency between 80-95% depending on the engine's operating conditions and air/fuel ratio as seen in the figure below.

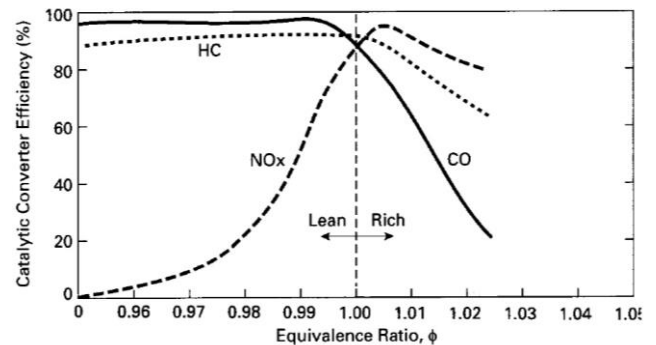


**Figure 6. Catalytic Converter Efficiency vs Air/Fuel Ratio**

Notice how efficiently the catalyst converts HC and CO when the equivalence ratio of the exhaust gases is below phi 1.00. Though NO<sub>x</sub> efficiency decreases significantly, the added EGR valve helps to improve this. As we said previously, our goal was to fall within that window of operation. Our equivalence ratio will drop to 0.95 during cruising speeds of 45 mph in order to improve the snowmobile's fuel economy. Though this allows us to save fuel, it also increases NO<sub>x</sub> particles. As seen on figure 7, decreasing the value of phi causes a reduction in HC and CO particles, but an increase in NO<sub>x</sub>.

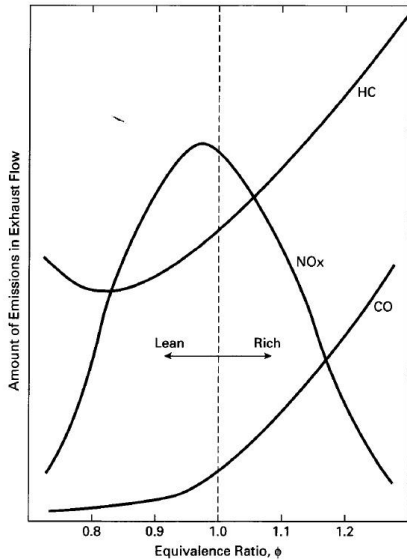


Figure 7. Amount of Emissions in Exhaust Gases vs Air/Fuel Ratio

A test was run to show the effects of running an engine lean on its NOx emissions. The tests were carried out at an engine speed of 3500 RPM and with a 30% throttle position opening.

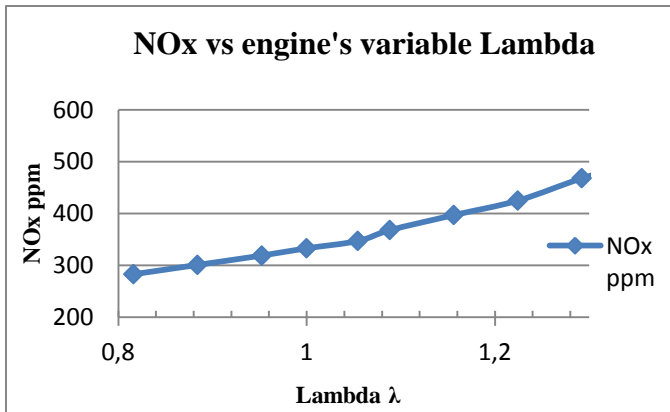


Figure 8. NOx ppm vs Engine Lambda of operation (at 3500 RPM at 30% TPS)

By observing the results illustrated on figure 8, we can conclude that air fuel ratio is directly proportional to NOx emissions. As seen in figure 6, the catalytic converter will still be efficient for HC and CO particles with a lean burning engine but conversion efficiency for NOx will drop drastically. Looking at NOx formation, we can identify three sources contributing to its formation. The first and major source of NOx formation is due to heat peaks in the combustion chamber. The second source is due to the reaction of nitrogen with hydrocarbon radicals. The last source of NOx formation is due to the nitrogen found in the fuel itself. Since the heat peaks in the combustion chamber are considered the most significant source for NOx formation, a consideration was taken to eliminate the two other sources and working on

reducing the flame temperature of the combustion. By looking at figure 9 which illustrates the Zeldovich NOx formation model, we can observe the direct link to flame temperature and NOx formation rate.

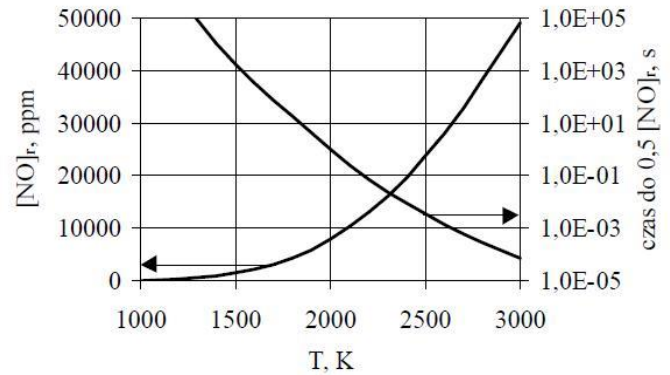
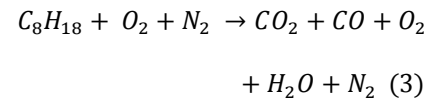


Figure 9. NOx ppm vs flame temperature (NOx formation according to the Zeldovich model)

With such a comparison, the inevitable solution for this problem would be to implement an EGR system in order to reduce the combustion flame temperature. By re-circulating a certain percentage of the exhaust gases, the quantity of oxygen available for the combustion is reduced and replaced with inert gases such as CO and CO2. To be able to get the approximate quantity required, a comparison method is used to calculate the amount of energy on the reactive side of the combustion chemical equation versus the amount of energy on the product side of the equation.



By using the first rule of thermodynamics, a balanced energy equation can be established. For this comparison method, we consider that there is no work exchanged (W), no kinetic energy (Ek), no potential energy (Ep) and no heat exchanged with surrounding environments (combustion chamber).

$$Q - W = \Delta E = \Delta H + \Delta E_c + \Delta E_p \quad (4)$$

$$\Delta E = \Delta H \quad (5)$$

$$\Delta E = H_{product} - H_{reactive} \quad (6)$$

What we have left is the difference between the enthalpy of the reactive and the enthalpy of the products. In other words, the enthalpy of the products is equal to the enthalpy of the reactive.

$$H_{product} = H_{reactive} \text{ (Units kJ/kmol)} \quad (7)$$

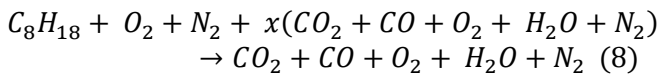
$$\begin{aligned} [\sum np (h^{\circ f} + (h - h^{\circ}))_{product} \\ = \sum nr (h^{\circ f} + (h - h^{\circ}))_{reactive}] \end{aligned}$$

We can now work with the equation above to compare the enthalpy by estimating a combustion flame temperature for the reactive. We have  $h^{\circ f}$  representing the formation enthalpy of the molecules,  $h$  represents the enthalpy of a molecule at a known temperature and  $h^{\circ}$  represents the enthalpy at a reference temperature. By starting with a flame temperature of 1600 K, we can assume that the actual temperature will be much higher, therefore, it is possible to iterate to a higher flame temperature until the enthalpy of the products is equal to the enthalpy of the reactive. This temperature will give us the peak temperature of the combustion for a given combustion formula.

**Table 2. Theoretical Adiabatic Fuel Temperature (K)**

TPS (%)	40	1620	1680	1600	1580	1560	1560
	35	1620	1680	1600	1600	1560	1560
	30	1620	1660	1580	1580	1560	1560
	25	1620	1660	1580	1580	1560	
	20	1600	1640				
	15	1600					
		3250	3750	4500	4750	5250	5500
		RPM					

In table 2, we can find the theoretical adiabatic flame temperature of combustion for the operating cells of the EGR valve. With these temperatures, we can now fix a reduction objective which in our case is 200K. The new combustion equation with re-circulated gases is as described below with  $x$  representing the percentage of gases re-circulated.



The actual quantity of exhaust gases re-circulated is determined with the difference in pressure between the intake of the EGR valve and the out port, and the EGR valve position. By using Bernoulli's equation of energy, we can isolate the fluid speed variable which will vary with the valve's position.

$$\begin{aligned} Z_1 + \frac{P_1}{\gamma} + \frac{v_1^2}{2g} + H_p - H_m - H_L \\ = Z_2 + \frac{p_2}{\gamma} + \frac{v_2^2}{2g} \quad (9) \end{aligned}$$

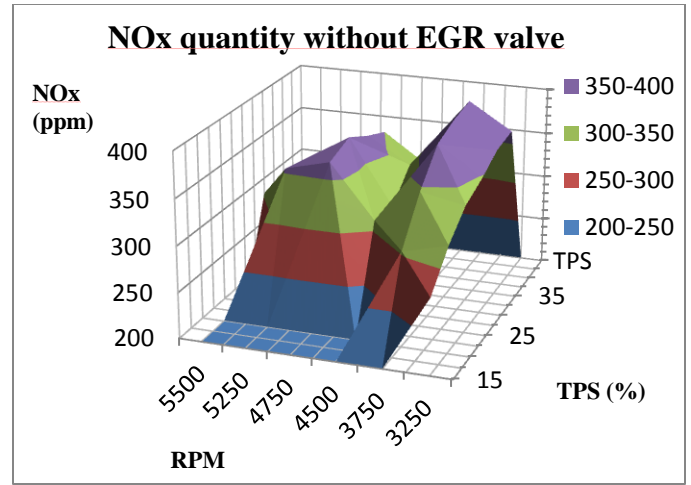


**Figure 10. NOx Quantity without EGR Valve**

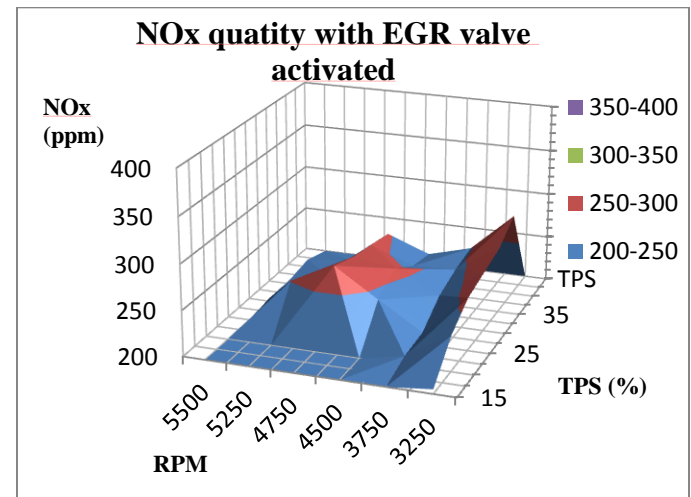


**Figure 11. NOx Quantity with Active EGR Valve**

By comparing figure 10 and 11, the effects of the EGR valve on NOx have been proven very effective. The achieved global NOx reduction of 23% in the EGR's operating range proves that the reduction in the flame temperature is directly linked to the reduction of NOx.

Following the emissions data collection, a rise in HC particles and a loss in power were noticed. The air fuel ratio also dropped resulting in a rich combustion. To explain these variances, the following equation representing the flame's front speed shows the effects of re-circulated gases.

$$S_L(x_b) = S_L * (1 - 2.06 * x_b^{0.77}) \quad (10)$$

Where  $S_L$  is the flame speed and  $x_b$  is the percentage of re-circulated gases. With a greater quantity of re-circulated gases, the flame speed reduces. To compensate, more spark advance is needed to allow more complete flame propagation and to be able to harvest the maximum amount of power from the fuel.

## Turbo selection

Our engine setup features an intercooled Garrett turbocharger. We upgraded from our previous GT1241 to an MGT1238Z. In fact, after some calculations, it was determined that the MGT1238Z fit better with the desired operating range of our engine. We planned for the future and set the limit our team would like to achieve one day to 110hp at 7250 rpm. To achieve this power the old turbo would have to spin way passed its max speed limit of 220000 rpm. The new setup has the potential to rotate up to 295000 rpm. To achieve the desired power goal, it has to work just below this limit, as seen on figure 12. This gives us a proper safety margin to work with our ultimate goal while also providing fast spool.

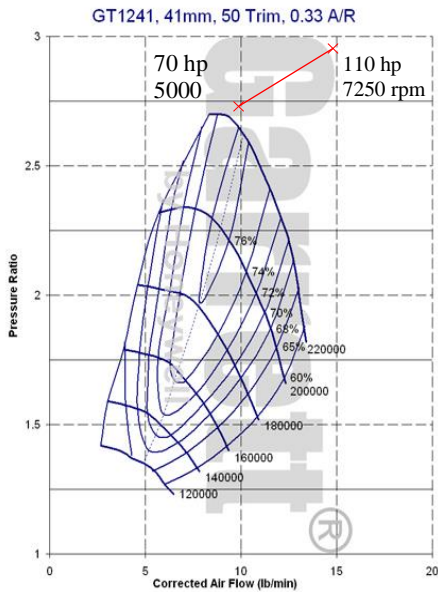


Figure 12. GT1241 Compressor map

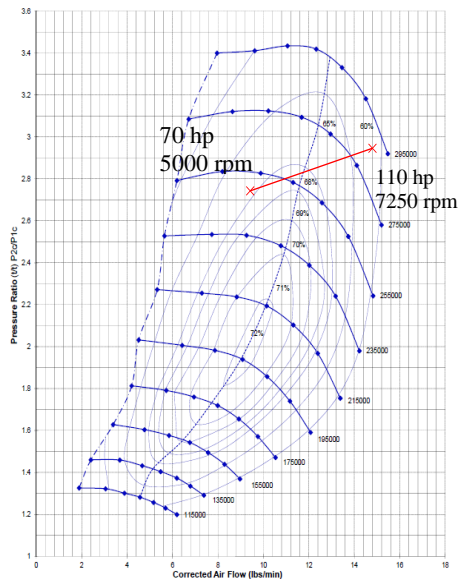


Figure 13. MGT1238Z Compressor map

## Electronic throttle control

The installation of an electronic throttle control is one of many upgrades done on our snowmobile this year. Also known as drive-by-wire system, this throttle body is actuated by an electric signal from the engine management system, which receives data from the throttle lever. An electronic throttle control is more efficient compared to the previous mechanical throttle control. It is also capable of controlling engine idle speed, replacing the auxiliary idle valve originally needed on a mechanical setup. The throttle lever is softer and easier to operate improving driver's comfort. This system allowed us to program the ramp of the throttle opening, resulting in a smoother power delivery. This, once again, helps improve maneuverability, an important concern for our team.

## Intercooler duct

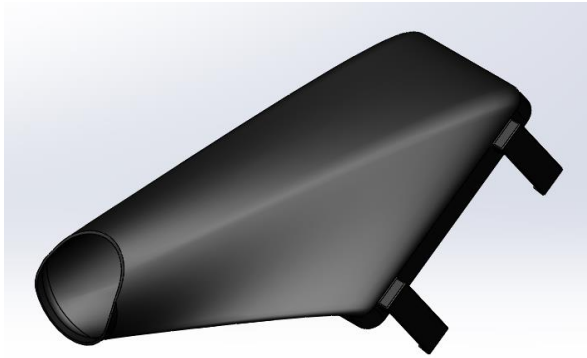
Last year, we changed the configuration of our charged air cooling system from a front mounted intercooler to a top mounted one (see figure 14). We did this for several reasons. First and foremost, to gain space in the front of the engine bay in order package more components in this tight area. We also favored the shorter piping with less bends this arrangement allowed. The results we were looking were quickly confirmed. However, one major drawback was observed. Since, by design, this configuration limits the air that passes through the intercooler, the cooling efficiency of the intercooler was dramatically reduced. Since the fins are so restrictive, the air that travels into the engine compartment and to the intercooler simply deviates past it because it follows the least restrictive path.



Figure 14. Top mounted intercooler

The solution we found to be most promising was to use the factory hole in the top cab and direct the entirety of the air to the intercooler using a 3D printed PEI plastic duct. This material is specifically designed to reflect heat and withstand high ambient temperatures (rated for continuous operation at 150°C). The duct uses CAD designed curves to smoothly guide the cold exterior air onto the intercooler while allowing the cab to retain a factory look. This way, the intercooler, which is heated by the ambient air of the engine bay, has some fresh air forced passed its cooling fins. Though, at the time of this writing the part isn't yet finished being fabricated, we expect great results and will certainly demonstrate its

effectiveness in future papers. Figure 15 shows the CAD model of the said part.



*Figure 15. CAD model of the intercooler duct*

### Heat management

To insure good reliability and performance, emphasis was put on heat reduction and protection. The wires and oil and coolant lines surrounding the exhaust and turbocharger are protected by a high heat braided ceramic sleeve. Heat reflective tape was installed on the intercooler and intake pipes to reduce their heat absorption. This particular tape is made of a polyamide ceramic glass cloth and aluminium sheet and is specifically designed to reduce the effect of radiant heat.

The exhaust manifold is now wrapped in a ceramic cloth and is also equipped with a stainless steel heatshield that proved to be particularly effective. We saw a reduction of as much as 280°F between the surface of the exhaust wrap and the surface of the heat shield.

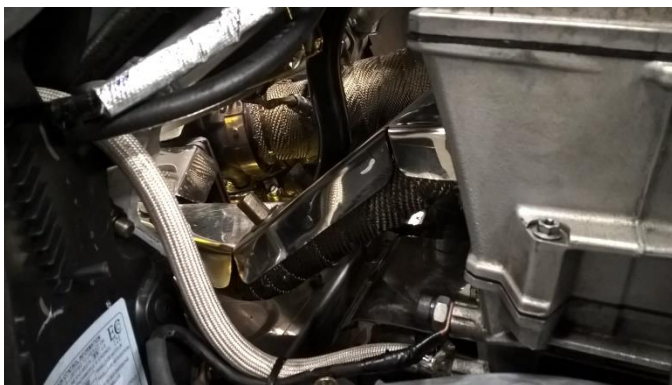


*Figure 16. Exhaust manifold's wrap and heatshield*

Several other heat shields are placed in the engine bay to insure the higher ambient heat caused by the turbo doesn't cause additional stress on the temperature sensitive components. All these simple precautions help us manage the heat in the engine compartment and help prevent failures.

## ACOUSTICS AND NOISE REDUCTION

### Exhaust Design

This section examines more thoroughly the thought process behind the design of the exhaust system. For the most part, this year's product is based on last year's concept. Since the previous exhaust yield good improvement over stock, it served as a base for the new system.

The casing of the new muffler is very similar to the previous one. As a matter of fact, only minor exterior modifications were made in order to improve fitting of the part in the snowmobile as well as facilitate its assembly. Some examples of the improvements implemented include, but are not limited to: dimension constraints, substitution of wide radius bends for simple bends, addition of bends in some strategic points in order to limit welding, etc. The biggest alteration to the design is the fact that the front panel is now removable. This allowed us, during testing period, to properly examine the quality of the absorbent material used; improper isolation was a major flaw we encountered during last year's competition.

The external panels were altered for faster and simpler construction which resulted in an overall lighter muffler. The method used is a simple sheet interlock and folding tabs of the various parts making it easier to assemble with a lot less welding.

The following figures compare the previous version of the muffler with the new one.

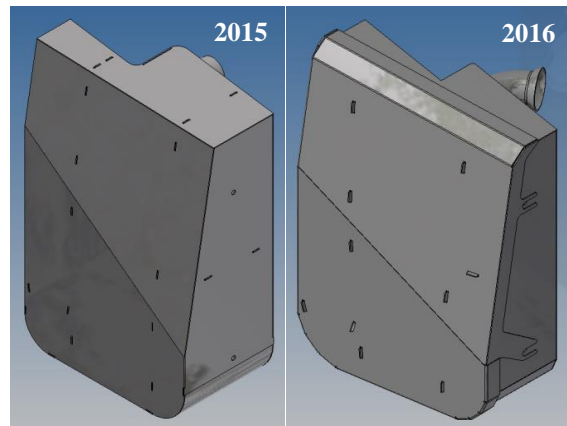


*Figure 17. New and Old Exhaust Muffler Design*

The interior of the silencer is also very similar to that of last year's. Exhaust gases follow the same path through the various sections. However, the replacement of many wall separators with perforated plates allow a more efficient noise reduction from the areas filled with sound deadening packing material. The middle section resonator was revised in order to



allow adjustments of the aimed frequencies. The three small horizontal pipes are now threaded and adjustable to allow for a resonator pre-set and fine adjustments.

The length of each resonator has been determined experimentally in order to mitigate the desired sound frequencies. This being said, the more present 600Hz, 700Hz and 850Hz are now greatly dampened. Furthermore, the slight design rework allows the elbow at the entry of the muffler to serve as an additional resonator. Sections 1, 2 and 3 are purposely filled with sound dampening material in order to lessen the noise generated by the entire frequency range. This process performs significantly well with higher frequencies. Figure 18 illustrate the interior design of the latest exhaust muffler.

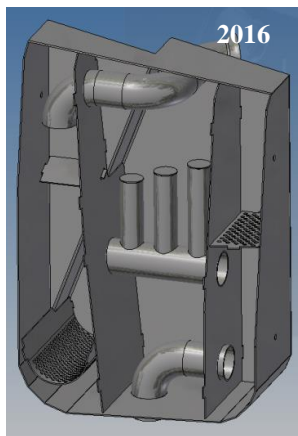


**Figure 18. Muffler's Interior Design**

With the sole purpose of optimizing the length of the resonators and reducing noise, many acoustic tests were performed on the motor. These measurements were conducted on an exhaustless engine at various rotation speeds (from 4000RPM to 7000RPM by increments of 500RPM). The 3D graph from figure 30 in the Appendix C points out these results. These results indicate that the engine generates most of its strong frequencies between 150 Hz to 900 Hz (see Appendix B for details). By adjusting the resonator's length, it will be possible to increase the exhaust system's efficiency and eliminate the targeted frequencies.

A simple equation allows us to determine the necessary length of a resonator in order to eliminate the desired frequencies:

$$f = \frac{c}{4 * L} \quad (11)$$

However, in practice there is a phenomenon called edge effect which slightly distorts the expected results. Indeed, the edge of a resonator influences the path of a wave in a way that simulates a longer tube length than what it really is. Thus, to counter this deviation, the resonator must be slightly shorter than what the theoretical value suggests. Table 3 in Appendix A shows the difference between speculated theoretical

frequencies and experimentally observed frequencies for the resonators present in the exhaust system.

The substantial difference between the expected and obtained results is what encouraged us to modify the sound reduction system of the exhaust. Thereby, we were able to match the desired frequencies by adjusting each resonator's length inside the muffler and therefore increase its efficiency. It wasn't possible to experimentally measure the frequency in the resonator at the entry of the muffler which explains why it wasn't modified.

Finally, we ran new tests with the new exhaust fitted to the engine and were able to achieve the results found in the 3D graph from figure 31 in Appendix C. On a global point of view, the noise level is reduced throughout the entire sound stage. Moreover, it seems that engine speed only slightly affects noise intensity. It is nonetheless hard to quantify noise reduction by simply comparing the figure 30 and figure 31. Thus, the figure 19 shows the logarithmic difference between the exhaustless engine and the one fitted with this year's exhaust.

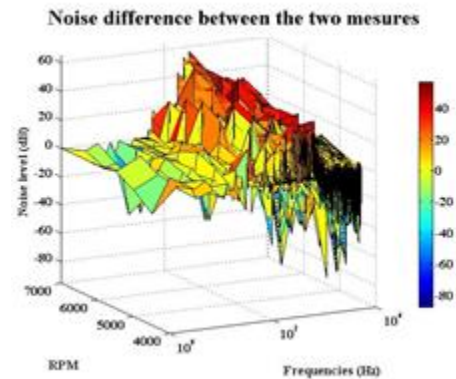


**Figure 29. Noise Reduction from 2016 Exhaust**

The exhaust seems to be more effective in the 200 to 1000Hz range, which specifically corresponds to the loudest zone of the sound stage. Therefore, the resonators and absorption chambers have adequately been optimised. However, the major improvement noticed in the 200 Hz range remains unexplained, since our sound reduction methods did not aim this frequency. It would be important and even necessary to push our research a step further in order to understand which element affects this particular frequency.

### Air intake

With the same optic of reducing noise from the previous prototype, a new air intake was designed for this year's prototype. We previously noticed a fair amount of sound emerging from the front part of the snowmobile so drastic changes were needed from the previous design, which didn't have noise reduction features. The air entry was relocated and we added an expansion chamber in between the air filter and the turbo inlet. This chamber was added to the air intake pipe

and its simple design essentially consists of a 5.5" diameter by 7" long cylinder inlet and outlet. An inlet to connect to crankcase vent and an inlet to connect to the bypass valve are also integrated to the expansion chamber. It is also filled with sound absorbing foam to reduce the noise from the air induction and bypass valve. Its body is 3D printed in PEI plastic to keep the whole assembly lightweight and heat reflective.

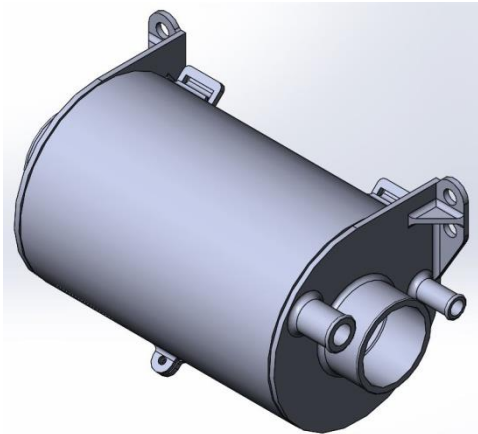


*Figure 20. Air intake expansion chamber*

## Noise Trap Vent

The engine compartment was revised for the new prototype as last year's sound data showed many easily identifiable engine noises. It was also found that one of the big sound sources was the 5" by 11" air vent on the snowmobile's front end. In order to keep the engine noises inside as much as possible without affecting the air flow through the engine compartment too much, a noise trap was added. It consists of 45° fins with a flat end on which sound waves from the engine and turbo will rebound. To compensate for the reduction in airflow occurred by the trap, the air intake entry was moved to the side of the cab to keep maximum air flow for cooling. To keep weight as low as possible, this part is 3D printed in plastic. Combined with the new air intake design, we measured a 100dB sound level reduction 5" from the air vent.



*Figure 21. Front grill noise test*

## Track Tunnel Soundproofing

Noise made by the moving track is a major noise source on a snowmobile. Actions taken to reduce the amount of noise coming out of the tunnel consist in the addition of a sound deadening patch layer on the whole inner section and the installation of a rubber skirt that acts as an extension to the snow flap. The sound deadening material used is Henkel's Terophon 231000. It's made from a butyl rubber base layer with a thin aluminum foil on top and has the purpose to keep the tunnel's aluminum shell from vibrating from the sound waves coming from the moving track so they just rebound inside the tunnel. The skirts are made from neoprene and are a compromise between full length skirts, which would keep most of the noise inside the tunnel but would have the disadvantage of trapping the snow inside the tunnel and being aesthetically unappealing, and no skirts at all. They are long enough to reduce the opened area under the tunnel but subtle enough not to disturb the snowmobile's look.

## Track Test bench and Noise Analysis

For the past years, Club QUIETS has successfully designed exhaust systems that reduce noise to a point where the track becomes the major noise source of the snowmobile. With this in mind, the club has decided to build a test bench for which the sole purpose is to study this aspect. The project being established on a long term base, this year's objective was to build the test bench and conduct the first sound tests.

The test bench consists mainly of a steel structure that supports the chassis of the snowmobile. It is held by the front suspension mounting points as well as by the rear reinforcement bar. The structure itself is equipped with auto blocking wheels that allow the bench to be moved around easily. An electric motor is located where the combustion engine usually sits and it drives a belt. A hinge holds the motor in place and uses the weight of the motor to properly tension the belt. Finally, the belt transmits the power directly from the motor to the track's sprocket. Figure 22 shows the test bench while fitted with the drive system.

Since sound tests have a great importance in the competition, we have decided this year to focus on the noise made by our snowmobile. We started out on the sound test bench that was built in past years. We solidified it to reduce the bias caused by vibrations from the frame which supports the snowmobile's chassis. We also installed rubber pads to improve its stability. We added a belt (similar to what can be found on a conveyor) under the track to compress the suspension, thus representing realistic riding conditions.



Figure 22. Acoustic test bench

Nevertheless, the tests were not conclusive since the electric motor was not powerful enough to run the conveyor belt. This being said, we reverted to the setup we used in the past which involves spinning the track without restriction. All the tests were made according to a strict protocol to ensure the repeatability of our results. For example, the snowmobile was in the same position to maintain the same distance with the microphone each time. Also, the speed of the electric motor was controlled by a drive to ensure a constant cruising speed of 30mph.

This test bench allowed us to analyse different components and pieces, and identify which were best for noise reduction. This year, we wanted to compare the differences between the OEM wheels and some machined aluminum wheels, as well as the adjustment of the tension on the track (using the adjustment knob on the suspension). We also wanted to see the impact of anti-stabs, which are the small wheels located on the front suspension, to the noise and consumption. The following graphs display the results.

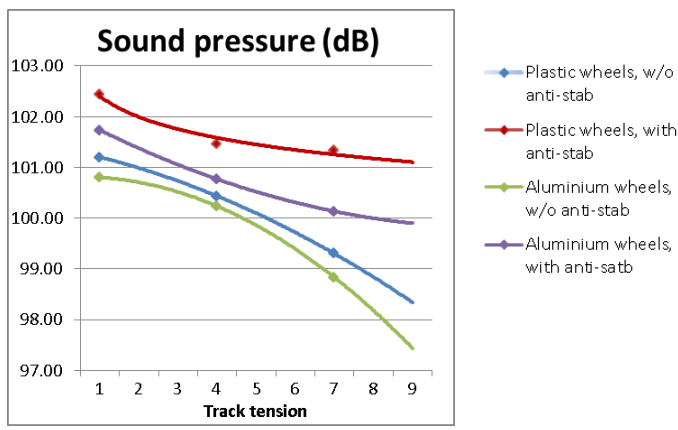


Figure 23. Variation of sound pressure with track tension

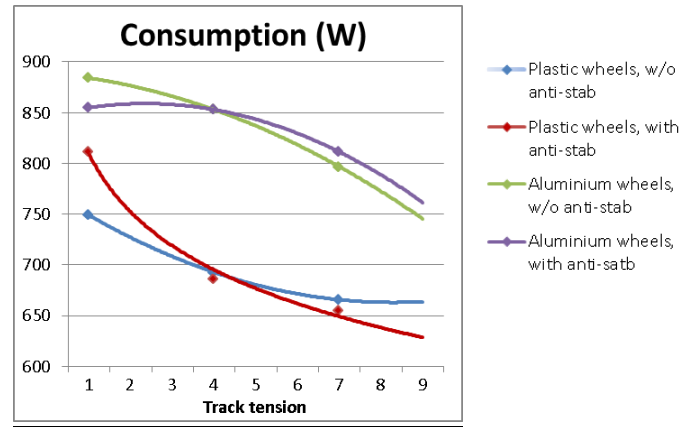


Figure 24. Variation of power consumption with track tension

You can see the different results we have obtained in the figures 23 and 24. It is important to consider these results are relative to each other and not absolute. This allowed us, nonetheless, to compare the effects of the changes we made.

Following these results, we have performed several tests with the snowmobile in real conditions to validate the data obtained on the test bench. These tests were based on a subjective comparison of the noise level and were performed as specified in the rules of the competition. The results were similar to what we measured on the test bench.



Figure 25. Sound test performed outside as per the competition's rules

We noted that the use of aluminum wheels reduced the noise but increased fuel consumption, which is why we decided to install rear wheels of a larger diameter, thus increasing the radius of curvature which had for effect to decrease the resistance of rotation. The following formula describes the effect of this theory.

$F = \frac{\pi}{2} \times \frac{1}{W} \times \frac{E'' \times I}{P_0^2}$	<p>F : drag force  W : load  E'' : dynamic modulus  I : inertia of belt section  Po : radius of curvature</p>
--------------------------------------------------------------------------	-------------------------------------------------------------------------------------------------------------------------------

Finally, according to the results, the best setup is to keep the manufacturer recommended tension and to change to aluminum wheels.

## **SUMMARY/CONCLUSIONS**

The design of our new four-stroke turbocharged engine is an exciting step for team QUIETS. Since the turbocharged 600ACE has already shown its potential, we can proudly say that our innovations are still going further. The implementation of a modified intake and exhaust manifolds, improved exhaust muffler design, simplified wire harness and an efficient EGR valve put this sled ahead of stock model regarding efforts to offer maximum performances, while reducing noise and exhaust emissions. Our few years of tests and experience with turbocharged snowmobiles lead us a step forward in the right direction toward the design of an eco-friendly, yet powerful snowmobile.

## **REFERENCES**

1. Çengel, Y.A., Boles, M.A. "Thermodynamics: An Engineering Approach", 8 Edition, McGraw-Hill, Montréal.
2. Çengel, Y. A. & Cimbala, J. M. 2014 "Fluid Mechanics: Fundamentals and Applications", 3rd Edition, McGraw-Hill, New-York.
3. Levendis Y A, Pavalatos I, Abrams R F "1994 Control of diesel soot hydrocarbon and NOx emissions with a particular trap." SAE Technical Paper 940460
4. Miller, J. and C. Bowman. "Mechanism and modeling of nitrogen chemistry in combustion: Prog Energy" Combustion. Sci. 15, 287-338, 1989
5. Willard W. Pulkrabek, «Engineering Fundamentals of the Internal Combustion Engine», University of Wisconsin: Prentice Hall
6. Allen V., Reicks. 2012. "A Comparison of Calculated and Measured Indentation Losses in Rubber Belt Covers". Online. 18 p.  
[http://overlandconveyor.com/pdf/bsh\\_003\\_2012\\_reicksa\\_conveyor.pdf](http://overlandconveyor.com/pdf/bsh_003_2012_reicksa_conveyor.pdf). Consulted February 18 2016.

## **DEFINITIONS/ABBREVIATIONS**

CO	Carbon Monoxide
CO2	Carbon Dioxide
EGR	Exhaust Gas Re-circulation
EGT	Exhaust Gas Temperature
EMS	Engine Management System
HC	Hydro Carbon
H2O	Hydrogen Dioxide
Hz	Hertz
MPH	Miles per hour
NOx	Different groups of nitrous oxides
RPM	Rotations per minute
AKI	Anti-knock index, also known as PON (Posted Octane Number)

**APPENDIX A**

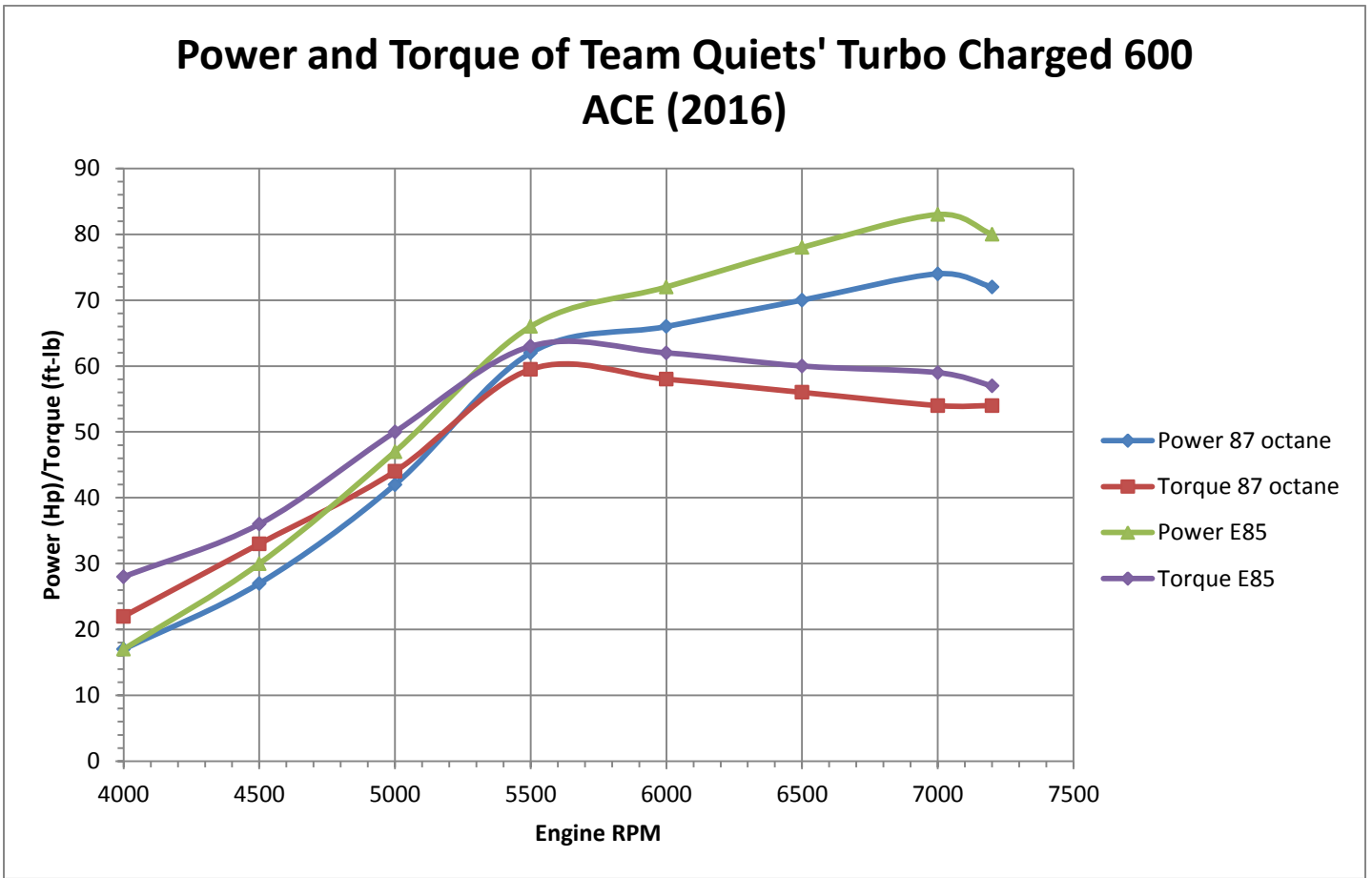


*Figure 26. Power and torque curves for 2016*

# APPENDIX B

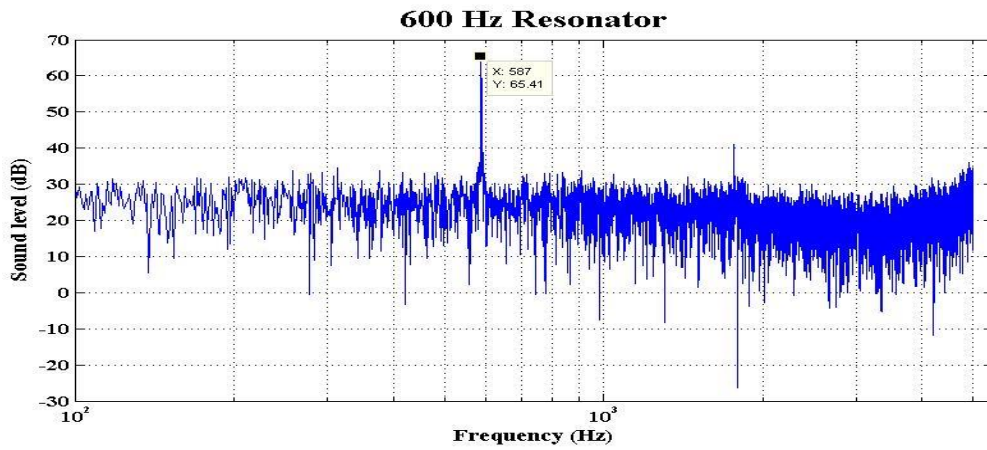


Figure 27. Resonator for 600 Hz

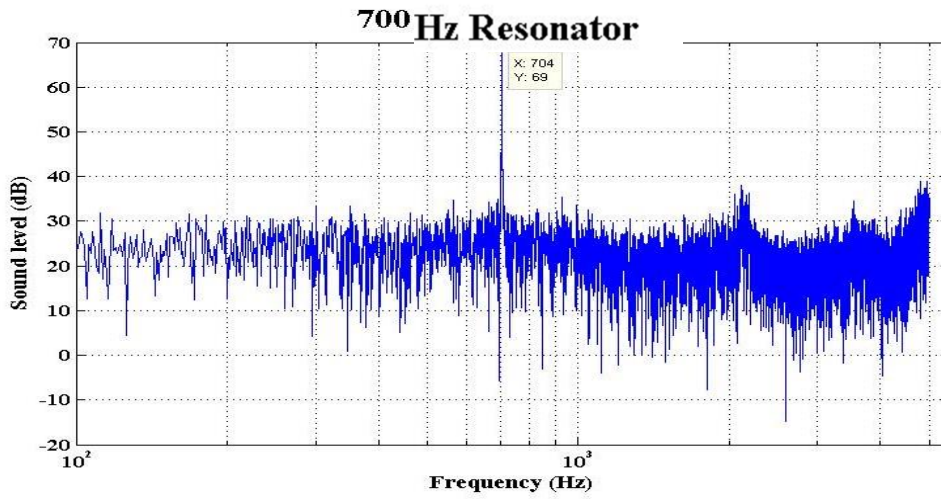


Figure 28. Resonator for 700 Hz

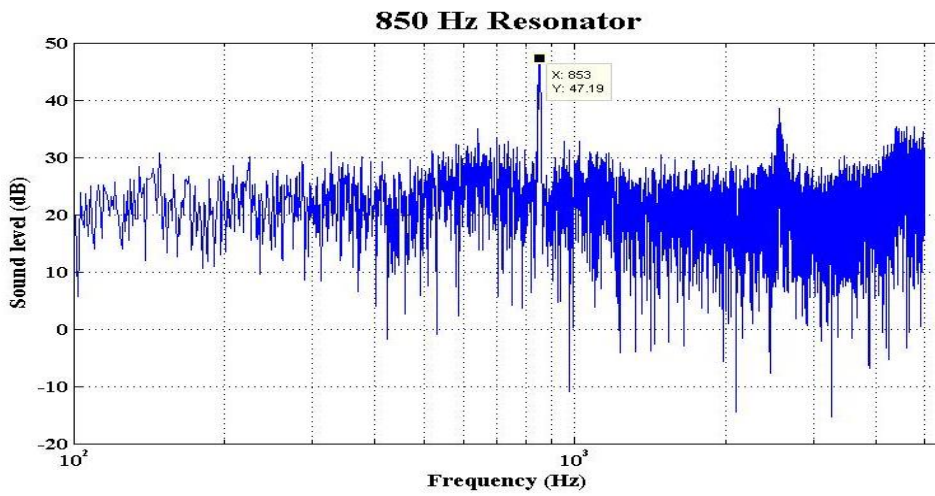
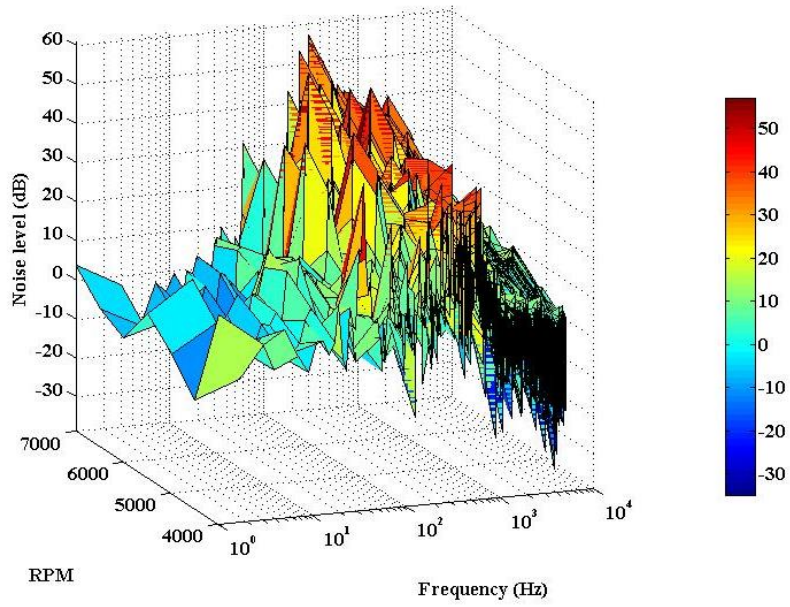


Figure 29. Resonator for 850 Hz

# APPENDIX C

**Noise level vs frequencies and RPM (straight)**



*Figure 30. Engine Noise Level without a Muffler*

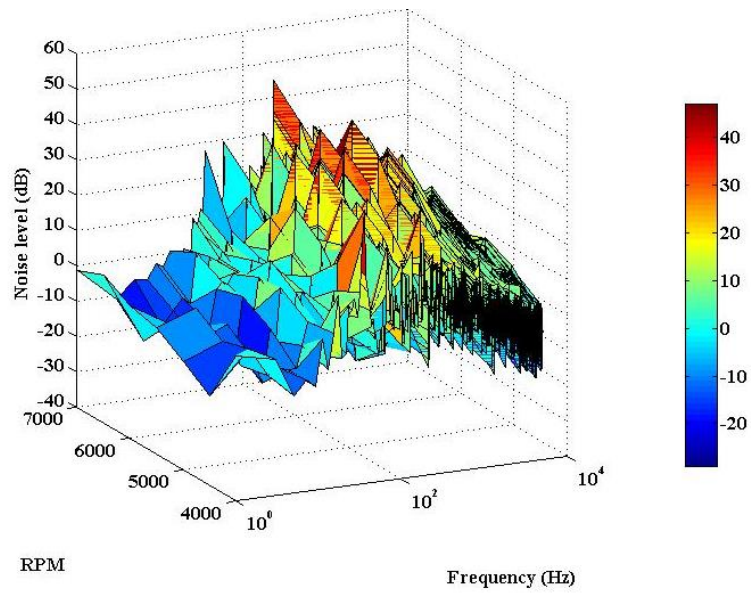


*Figure 31. Engine Noise Level with 2016 Exhaust System*